# Theoretical study of potential energy curves, spectroscopic constants, and radiative lifetimes of low-lying states in an SeO molecule*

Li Rui(李 瑞)[a)b)], Lian Ke-Yan(连科研)[a)], Li Qi-Nan(李奇楠)[b)], Miao Feng-Juan(苗凤娟)[c)], Yan Bing(闫 冰)[a)†], and Jin Ming-Xing(金明星)[a)]

[a)] *Institute of Atomic and Molecular Physics, Jilin University, Changchun* 130012, *China*

[b)] *Department of Physics, College of Science, Qiqihar University, Qiqihar* 161006, *China*

[c)] *College of Communications and Electronics Engineering, Qiqihar University, Qiqihar* 161006, *China*

(Received 3 April 2012; revised manuscript received 20 June 2012)

The low-lying potential energy curves of the SeO molecule are computed by means of an *ab initio* multireference configuration interaction technique, taking into account relativistic (scalar plus spin–orbit coupling) effects. The spectroscopic constants of Ω states for $X^3\Sigma^-$, $a^1\Delta$, $b^1\Sigma^+$, $A^3\Pi$ , $A'^3\Delta$, and $A''\ ^3\Sigma^+$ states are obtained, and they are in good accordance with available experimental values. The Franck–Condon factors and transition dipole moments to the ground state are computed, and the natural radiative lifetimes of low-lying Ω states are theoretically obtained. Comparisons of the natural lifetimes of Ω states with previous experimental results and those of isovalent TeO molecule are made.

**Keywords:** potential energy curves, spin–orbit coupling, lifetime, SeO molecule

**PACS:** 31.50.Df, 31.15.aj, 31.15.ag **DOI:** 10.1088/1674-1056/21/12/123102

## 1. Introduction

Selenium (Se) is one of most valuable rare elements because it is an essential nutrient for the human body and it is also one of important elements in biological chemistry. The bonded and nonbonded interactions between oxygen (O) and selenium have aroused much theoretical and experimental research interest.[1] Similar to molecular oxygen ($O_2$), the selenium monoxide, i.e., the SeO molecule, exhibits rich optical spectra, which can provide a great deal of information about the SeO molecule. The rotational energy levels and vibrational energy levels of a SeO molecule can be directly deduced from molecular optical spectra, and the geometrical structures of the ground state and the excited state of a SeO molecule can also be obtained with optical spectra. As a result, the optical properties of SeO molecules have attracted great attention in fundamental physics and biological chemistry.[2−4] During the past four decades, a large number of experimental studies have been reported on the spectra of SeO molecules and other related molecules.[5−10] The emission electronic band systems from the low-lying states $a^1\Delta$ and $b^1\Sigma^+$ to the ground state $X^3\Sigma^-$ were investigated by employing microwave discharge in a mixture of a He carrier with $SeOCl_2$.[5] The experimental data[5] indicate that the (0,0) bands of $a^1\Delta \rightarrow X^3\Sigma^-$ and $b^1\Sigma^+ \rightarrow X^3\Sigma^-$ of SeO molecule are around 5238 $cm^{-1}$ and 9685.4 $cm^{-1}$, respectively. The (0,0) and (1,1) emission bands of $a^1\Delta \rightarrow X^3\Sigma^-$ of SeO molecule were observed at about 5200 $cm^{-1}$ by using the method of energy transfer from $O_2(a^1\Delta_g)$ to the ground state of SeO molecules.[4] The radiative lifetimes for $a^1\Delta$ and $b^1\Sigma^+$ states of SeO were computed by Matsushita *et al.*[9] and Chattopadhyaya *et al.*[10] using *ab initio* calculations. The calculated radiative lifetimes for $a^1\Delta$ state in the above two references are 1.1 s and 1.4 s, respectively. The computed radiative lifetimes for $b^1\Sigma^+$ state in the above two references are 4.7 ms and 10.93 ms, respectively. However, there are few theoretical studies that have provided the potential energy curves (PECs) of a SeO

*Project supported by the National Magnetic Confinement Fusion Science Program of China (Grant No. 2010GB104003), the Fundamental Research Funds for the Central Universities, China (Grant Nos. 200903369 and 201103255), the Natural Science Foundation of Heilongjiang Province, China (Grant No. QC2011C092), and the Program for Young Teacher's Scientific Research in Qiqihar University, China (Grant Nos. 2010K-Z05 and 2010K-M31).

†Corresponding author. E-mail: yanbing@jlu.edu.cn

© 2012 Chinese Physical Society and IOP Publishing Ltd

molecule and the spectroscopic constants of low-lying states of a SeO molecule, with the spin–orbit coupling effects taken into consideration. Potential energy curves including spin–orbit coupling effects can provide more information about the transition properties between different electronic states of a SeO molecule. Hence, in order to better understand the molecular and spectroscopic properties of SeO molecules, the potential energy curves should be calculated, with the spin–orbit coupling effects taken into account. In the present work, we use an *ab initio* method to compute the PECs of the low-lying electronic states of a SeO molecule. In the PEC calculations, we consider the spin–orbit coupling effects with the Λ–S states interaction technique. According to the PECs, we further solve one-dimensional Schrödinger equations to obtain vibrational wavefunctions, Franck–Condon factors (FCFs), vibrational energy levels, and spectroscopic constants of bound states of the SeO molecule. Finally, we deduce the natural radiative lifetimes of low-lying bound states of the SeO molecule from calculated PECs and transition moments.

## 2. Method and computational details

In the present study, the electronic structure calculations are performed by using the Molpro2010 quantum chemical package.[11] The calculations are performed in $C_{2v}$ symmetry, where the $\Sigma^+$ is represented by $A_1$, $\Sigma^-$ is represented by $A_2$, and $A_1$+$A_2$ and $B_1$+$B_2$ represent degenerate states $\Delta$ and $\Pi$, respectively. The relativistic effective core potentials (RECPs) for Se and O atoms are employed to describe the scalar relativistic effects in combination with corresponding basis sets for valence electrons.[12,13] In order to improve calculation accuracy, the basis set of Se is augmented by one p polarization function, two d polarization functions, one f polarization function, and one 5s diffusion function with optimized exponents of 0.0328, 0.3630, 0.1330, 0.48000, and 0.039783, respectively; the basis set of O is augmented by three d polarization functions, two f polarization functions, and one 5s diffusion function with optimized exponents of 5.1600, 1.2920, 0.4225, 1.9000, 0.5000, and 0.0550, respectively. The PECs are calculated with highly correlated *ab initio* methods, namely, the complete active space self-consistent field (CASSCF) approach followed by the internally contracted multireference configuration interaction method (MRCI) with Davison size-extensivity correction (+Q).[14−16] As is well known, the low-lying excited states arise from excitation of valence electrons into empty valence orbitals. Hence, in the CASSCF calculations, the active space is made up of 4s, $4p_x$, $4p_y$, $4p_z$ valence orbitals of Se, 2s, $2p_x$, $2p_y$, $2p_z$ valence orbitals of O, and an additional $\sigma$ outer-shell orbital. So in the MRCI+Q calculations, all 12 valence electrons are correlated. The spin–orbit coupling effects are included in the electronic state calculations of the SeO molecule. The electronic dipole transition moments between the excited states and the ground state for SeO are also computed at the spin–orbit coupling (SOC) level. Sets of spectroscopic constants and wave functions of the bound Ω states are then deduced using a level program[17] to solve the one-dimensional Schrödinger equations. The Franck–Condon factor (FCF) from the vibrational level $v'$ of the upper electronic state to the vibrational level $v''$ of the lower ground state is obtained from the fitted PEC. The Einstein coefficient $A_{\nu'\nu''}$ between vibrational levels $v'$ and $v''$ is defined by

$$A_{\nu'\nu''} = 2.026 \times 10^{-6} \tilde{v}^3 (TM)^2 \left( \int \psi_{v'} \psi_{v''} \, \mathrm{d}r \right)^2 ,$$

where $\tilde{v}$ is the transition energy in units of $\mathrm{cm}^{-1}$, $TM$ is the average electronic dipole transition moment in Franck–Condon region in atomic units, and $\left( \int \psi_{v'} \psi_{v''} \, \mathrm{d}r \right)^2$ is the FCF between vibrational levels $v'$ and $v''$. The radiative lifetime of vibrational level $v'$ is given as the inverse of the total transition probability

$$\tau = \left( \sum_{v''} A_{v'v''} \right)^{-1} .$$

## 3. Results and discussion

### 3.1. Potential energy curves of SeO

The 18 Λ–S electronic states related to the lowest dissociation limit ($Se(^3P)$+$O(^3P)$) for a SeO molecule are computed at the MRCI+Q level. The $B^3\Sigma^-$ electronic state that dissociates into the second lowest dissociation limit ($Se(^1D)$+$O(^3P)$) is calculated at the same level. The PECs for the total 19 electronic states are shown in Fig. 1. These PECs are illustrated in energy relative to the minimum energy point of the ground state $X^3\Sigma^-$. Each PEC is constructed on 29 discrete points at a series of internuclear distances from $r$ = 1.29 Å (1 Å=0.1 nm) to $r$ = 3.6 Å. As shown in Fig. 1, nine of these Λ–S electronic states are bound, which are $X^3\Sigma^-$, $a^1\Delta$, $b^1\Sigma^+$, $c^1\Sigma^+$, $A'^3\Delta$, $A''^3\Sigma^+$, $A^3\Pi$, $1^5\Pi$, and $B^3\Sigma^-$. The $1^5\Pi$ state crosses the $A^3\Pi$ state at an internuclear distance of ∼ 2.2 Å,

and the crossing point is very close to the energy minimum ($r \approx 2.3$ Å) of $1^5\Pi$ state. Therefore, it is difficult to observe the $1^5\Pi$ state because of the perturbation of the $A^3\Pi$ state. Additionally, the crossing points will exhibit strong avoided crossings when the SOC interaction is taken into account, especially for $\Omega = 0$, 1, and 2. There are many crossings along the PEC of $B^3\Sigma^-$ state, in which the crossings with $1^5\Pi$ and $1^1\Pi$ states are energetically the lowest two at a internuclear distance of $\sim 2.0$ Å and $\sim 2.2$ Å, respectively. These crossings with repulsive or semi-bound PECs will make B–X transition more complicated when the spin–orbit interactions are introduced.

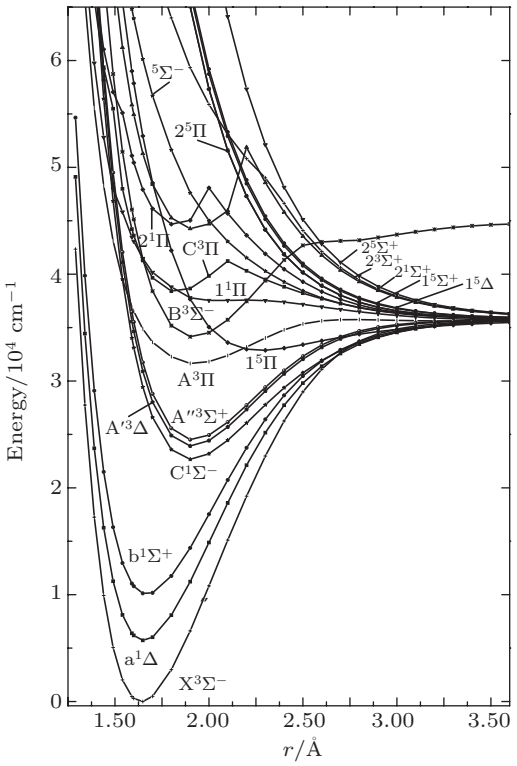



**Fig. 1.** Computed MRCI+Q potential energy curves for the low-lying electronic states of a SeO molecule, without the spin–orbit coupling effects taken into consideration.

The dominant electron configurations of the bound electronic states of SeO are given in Table 1. At the equilibrium distance of the ground state ($r = 1.65$ Å), all studied bound Λ–S states arise from the following three electronic configurations:

$$1 - 3\sigma^2 1\pi^4 2\pi^2, \tag{1}$$

$$1 - 3\sigma^2 1\pi^3 2\pi^3, \tag{2}$$

$$1 - 3\sigma^2 1\pi^4 2\pi^1 4\sigma^1. \tag{3}$$

The first configuration gives rise to three states ($X^3\Sigma^-$, $a^1\Delta$, $b^1\Sigma^+$), the second to four states ($c^1\Sigma^-$, $A'^3\Delta$, $A''^3\Sigma^+$, $B^3\Sigma^-$), and the third to one state ($A^3\Pi$). With the increase of internuclear distance $r$, the configuration with fully-occupied $2\pi$ orbital becomes important in the lowest three Λ–S states, which indicates that no electron transfer occurs in the dissociation of SeO ($X^3\Sigma^-$, $a^1\Delta$, $b^1\Sigma^+$). At an internuclear distance of $r = 2.2$ Å, the double electron excitation becomes prominent in $c^1\Sigma^-$, $A'^3\Delta$, $A''^3\Sigma^+$, $B^3\Sigma^-$ states. The transition from bonding $3\sigma$ orbital to antibonding $4\sigma$ orbital will lead to the increase of equilibrium bond length for these states. Similarly, the double electron excitation from $1\pi$ to $2\pi$ and $4\sigma$ orbital occurs in $A^3\Pi$ state at a longer bond distance. The transition of two electrons from bonding orbitals ($3\sigma$ and $1\pi$) to antibonding orbitals ($4\sigma$ and $2\pi$) causes a significant change (+0.3 Å) of bond length for excited states arising from configurations (2) and (3).

**Table 1.** Dominant electron configurations of low-lying electronic states of SeO for $r = 1.65$ Å and $r = 2.2$ Å.

| State | $r = 1.65$ Å | $\Sigma c_p^2$ | $r = 2.2$ Å | $\Sigma c_p^2$ |
|---|---|---|---|---|
| $X^3\Sigma^-$ | $(1\sigma)^2(2\sigma)^2(3\sigma)^2(1\pi)^4(2\pi)^2$ | 0.87 | $(1\sigma)^2(2\sigma)^2(3\sigma)^2(1\pi)^4(2\pi)^2$ | 0.62 |
| | | | $(1\sigma)^2(2\sigma)^2(3\sigma)^2(1\pi)^2(2\pi)^4$ | 0.14 |
| $a^1\Delta$ | $(1\sigma)^2(2\sigma)^2(3\sigma)^2(1\pi)^4(2\pi)^2$ | 0.85 | $(1\sigma)^2(2\sigma)^2(3\sigma)^2(1\pi)^4(2\pi)^2$ | 0.54 |
| | | | $(1\sigma)^2(2\sigma)^2(3\sigma)^2(1\pi)^2(2\pi)^4$ | 0.23 |
| $b^1\Sigma^+$ | $(1\sigma)^2(2\sigma)^2(3\sigma)^2(1\pi)^4(2\pi)^2$ | 0.81 | $(1\sigma)^2(2\sigma)^2(3\sigma)^2(1\pi)^4(2\pi)^2$ | 0.54 |
| | | | $(1\sigma)^2(2\sigma)^2(3\sigma)^2(1\pi)^2(2\pi)^4$ | 0.23 |
| $c^1\Sigma^-$ | $(1\sigma)^2(2\sigma)^2(3\sigma)^2(1\pi)^3(2\pi)^3$ | 0.96 | $(1\sigma)^2(2\sigma)^2(3\sigma)^2(1\pi)^3(2\pi)^3$ | 0.74 |
| | | | $(1\sigma)^2(2\sigma)^2(1\pi)^3(2\pi)^3(4\sigma)^2$ | 0.14 |
| $A'^3\Delta$ | $(1\sigma)^2(2\sigma)^2(3\sigma)^2(1\pi)^3(2\pi)^3$ | 0.95 | $(1\sigma)^2(2\sigma)^2(3\sigma)^2(1\pi)^3(2\pi)^3$ | 0.74 |
| | | | $(1\sigma)^2(2\sigma)^2(1\pi)^3(2\pi)^3(4\sigma)^2$ | 0.14 |
| $A''^3\Sigma^+$ | $(1\sigma)^2(2\sigma)^2(3\sigma)^2(1\pi)^3(2\pi)^3$ | 0.95 | $(1\sigma)^2(2\sigma)^2(3\sigma)^2(1\pi)^3(2\pi)^3$ | 0.74 |
| | | | $(1\sigma)^2(2\sigma)^2(1\pi)^3(2\pi)^3(4\sigma)^2$ | 0.14 |
| $A^3\Pi$ | $(1\sigma)^2(2\sigma)^2(3\sigma)^2(1\pi)^4(2\pi)^1(4\sigma)^1$ | 0.83 | $(1\sigma)^2(2\sigma)^2(3\sigma)^2(1\pi)^4(2\pi)^1(4\sigma)^1$ | 0.48 |
| | | | $(1\sigma)^2(2\sigma)^2(3\sigma)^2(1\pi)^2(2\pi)^3(4\sigma)^1$ | 0.32 |
| $B^3\Sigma^-$ | $(1\sigma)^2(2\sigma)^2(3\sigma)^2(1\pi)^3(2\pi)^3$ | 0.98 | $(1\sigma)^2(2\sigma)^2(3\sigma)^2(1\pi)^3(2\pi)^3$ | 0.74 |
| | | | $(1\sigma)^2(2\sigma)^2(1\pi)^3(2\pi)^3(4\sigma)^2$ | 0.14 |

The next step in the theoretical computation is to include the SOC effects in the SeO molecular Hamiltonian. The Hamiltonian of SeO including spin–orbit pseudopotential operator is solved in the basis of Λ–S MRCI wave functions and the calculated PECs of Ω states are shown in Fig. 2. The main distinctions of Fig. 2 are the splitting of Λ–S electronic states into their Ω components. The calculated dissociation energy $D_e$ for the ground state $X^3\Sigma_0^-$ is found to be 34870 $cm^{-1}$, and the spin–orbit coupling effect lowers the dissociation energy by 609 $cm^{-1}$ relative to that obtained at MRCI+Q Λ–S level. The Λ–S electronic state $B^3\Sigma^-$ split into $B_1^3\Sigma_0^-$ and $B_2^3\Sigma_1^-$ correlating to lower atom limits. The SOC effects lead to minor changes to the lower bound states; while for $B^3\Sigma^-$ state, the avoided crossings between Ω levels are found. As discussed above, the crossings between $B^3\Sigma^-$ and $1^5\Pi$, $1^1\Pi$ states in Λ–S PECs exhibit the avoided crossing nature in PECs of $\Omega = 0, 1$ components. Similarly, the avoided crossings along the PECs of $A^3\Pi$ occur at $\sim 2.2$ Å due to the perturbation of $1^5\Pi$ state.

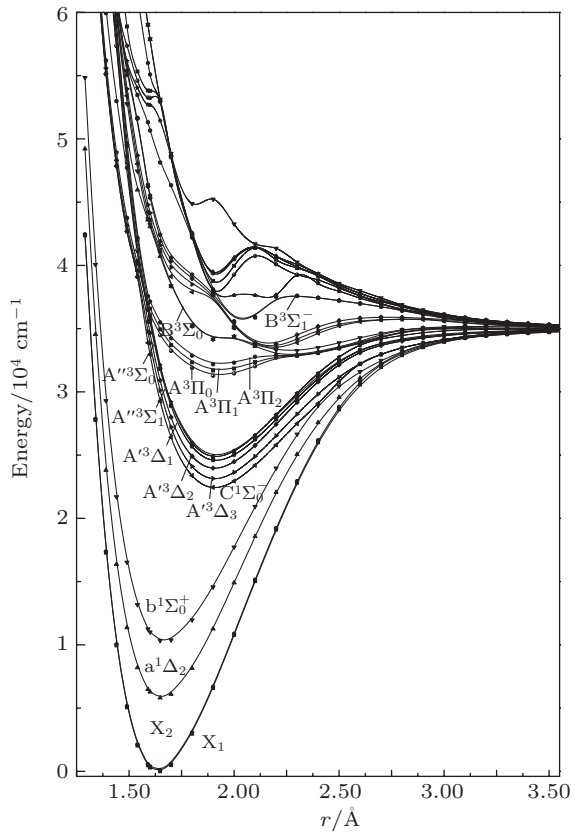



**Fig. 2.** Potential energy curves for the low-lying electronic states of the SeO molecule, with the spin–orbit coupling effects taken into consideration.

The compositions of low-lying states of SeO at different bond distances are shown in Table 2. Composition coefficients smaller than 0.6% are omitted in Table 2, but they are of importance for the accuracy of the transition moment. In the Franck–Condon region, the contribution of Λ–S state $X^3\Sigma^-$ to $X_1^3\Sigma_0^-$ is dominant; the admixture of $^1\Sigma^+$ character

**Table 2.** Compositions of Ω states of SeO ($c^2$,%) at different bond distances.

| State | $r$/Å | $^3\Sigma^-$ | $^3\Sigma^+$ | $^3\Pi$ | $^3\Delta$ | $^1\Sigma^-$ | $^1\Sigma^+$ | $^1\Pi$ | $^1\Delta$ | $^5\Pi$ |
|---|---|---|---|---|---|---|---|---|---|---|
| $X_1^3\Sigma_0^-$ | 1.6 | 99 | | | | | 1 | | | |
| | 1.7 | 98.8 | | | | | 1 | | | |
| | 2.0 | 98 | | | | | 1.8 | | | |
| | 2.2 | 96 | | | | | 4.0 | | | |
| $X_2^3\Sigma_1^-$ | 1.6 | 99.9 | | | | | | | | |
| | 1.7 | 99.9 | | | | | | | | |
| | 2.0 | 99.6 | | | | | | | | |
| | 2.2 | 98.9 | 0.6 | | | | | | | |
| $a^1\Delta_2$ | 1.6 | | | | | | | | 99.9 | |
| | 1.7 | | | | | | | | 99.9 | |
| | 2.0 | | | | 0.6 | | | | 99.1 | |
| | 2.2 | | | | 2 | | | | 97.5 | |
| $b^1\Sigma_0^+$ | 1.6 | 1 | | | | | 98.9 | | | |
| | 1.7 | 1.1 | | | | | 98.8 | | | |
| | 2.0 | 1.9 | | | | | 97.8 | | | |
| | 2.2 | 3.5 | | | | | 95.9 | | | |
| $c^1\Sigma_0^-$ | 1.6 | | 9 | | | 90.9 | | | | |
| | 1.7 | | 10.1 | | | 89.7 | | | | |
| | 2.0 | | 13.6 | | | 86.1 | | | | |
| | 2.2 | | 14.4 | | | 85 | | | | |
| $A_1'\,^3\Delta_3$ | 1.6 | | | | 99.9 | | | | | |
| | 1.7 | | | | 99.9 | | | | | |
| | 2.0 | | | | 99.5 | | | | | |
| | 2.2 | | | | 98.4 | | | | | 1.44 |
| $A_2'\,^3\Delta_2$ | 1.6 | | | | 99.7 | | | | | |
| | 1.7 | | | | 99.7 | | | | | |
| | 2.0 | | | | 99 | | | | 0.6 | |
| | 2.2 | | | | 96.8 | | | | 2 | 0.9 |
| $A_3'\,^3\Delta_1$ | 1.6 | | | | 99.6 | | | | | |
| | 1.7 | | | | 99.7 | | | | | |
| | 2.0 | | | | 99.3 | | | | | |
| | 2.2 | | | | 98.4 | | | | | 1 |
| $A_1''\,^3\Sigma_1^+$ | 1.6 | | 99.4 | | | | | | | |
| | 1.7 | | 99.8 | | | | | | | |
| | 2.0 | | 99.4 | | | | | | | |
| | 2.2 | | 99.4 | | | | | | | |
| $A_2''\,^3\Sigma_0^+$ | 1.6 | | 91 | | | 8.9 | | | | |
| | 1.7 | | 89.7 | | | 10.1 | | | | |
| | 2.0 | | 85.9 | | | 13.7 | | | | |
| | 2.2 | | 84.3 | | | 14.4 | | | | 1 |
| $A_1^3\Pi_0$ | 1.6 | | | 99.9 | | | | | | |
| | 1.7 | | | 99.9 | | | | | | |
| | 2.0 | | | 98.8 | | | | | | 0.9 |
| | 2.2 | | | 63 | | | 0.5 | | | 36.2 |
| $A_2^3\Pi_1$ | 1.6 | | | 99.2 | | | | 0.6 | | |
| | 1.7 | | | 99.2 | | | | 0.6 | | |
| | 2.0 | | | 97.7 | | | | 0.5 | | 1.4 |
| | 2.2 | | | 37.6 | | | | | | 61.4 |
| $A_3^3\Pi_2$ | 1.6 | | | 99.8 | | | | | | |
| | 1.7 | | | 99.8 | | | | | | |
| | 2.0 | | | 98.2 | | | | | | 1.5 |
| | 2.2 | | | 13.3 | | | | | 0.8 | 85.5 |

in $X_1^3\Sigma_0^-$ makes more electronic-dipole transitions to $X_1^3\Sigma_0^-$ state allowed. As bond distance $r$ increases, the character of $^1\Sigma^+$ becomes more prominent. The crossing point between the ground state and $b^1\Sigma^+$ at $r = 2.8$ Å (Fig. 1) becomes an avoided crossing point between $X_1^3\Sigma_0^-$ and $b^1\Sigma_0^+$, which indicates a strong coupling in the two Λ–S states at a long range of bond distance. The state mixing between the $X^3\Sigma^-$ and $A''^3\Sigma^+$ states results in $\Omega = 1$ component of the ground state $X^3\Sigma^-$. From Table 2, a large percentage (∼10%) of $A''^3\Sigma^+$ character is found in the $c^1\Sigma_0^-$ state, which is important for the transition property of the $c^1\Sigma_0^-$ state. The most striking feature in state composition is $R$-dependent coupling between the triplet Π state and the quintet Π state. The $^5\Pi$ character in Ω components of $^3\Pi$ is negligible for $r = 2.0$ Å, while for $r = 2.2$ Å the composition of the $^5\Pi$ character is over 36% for the $A_1{}^3\Pi_0$, 61% for the $A_1{}^3\Pi_1$, and 85% for the $A_1^3\Pi_2$. The $^3\Pi$ state is intensely perturbed through the admixture of the $^5\Pi$ character. The introduction of SOC relativity leads to obvious changes for low-lying excited states of SeO.

## 3.2. Spectroscopic constants

Based on the computed Ω-state potential energy curves, the spectroscopic constants of the SeO molecule are numerically obtained. The values of adiabatic transition energy $T_e$ of low-lying electronic state, equilibrium bond distance $r_e$, vibrational frequency $\omega_e$, and rotational constant $B_e$ are shown in Table 3. The adiabatic transition energies are computed as the differences between the energy minimum of the ground state and energy minima of the considered excited states. The SOC splitting of the ground state is computed to be 96.3 $cm^{-1}$, which is comparable to an experimental value of 165.9 $cm^{-1}$. The values of the theoretical $T_e$ of a and b are 5813 $cm^{-1}$ and 10274 $cm^{-1}$, respectively, which are reasonably in agreement with experimental values of 5300 $cm^{-1}$ and 9724 $cm^{-1}$, respectively. The calculated values of harmonic vibrational frequency $\omega_e$ of the $X_1^3\Sigma_0^-$, $X_2^3\Sigma_1^-$ states differ from the experimental results by 1.6% (∼ 15 $cm^{-1}$). The calculated $\omega_e$ of the $b^1\Sigma_0^+$ state is underestimated by 4% compared with experimental one. Our calculated vibrational frequencies for these states accord well with the experimental data. The values of rotational constant $B_e$ for the $X_1^3\Sigma_0^-$, $X_2^3\Sigma_1^-$, and $b^1\Sigma_0^+$ states are also in good agreement with experimental results, with an error of 0.061 $cm^{-1}$. The values of equilibrium bond distance $r_e$ for the $X_1^3\Sigma_0^-$, $X_2^3\Sigma_1^-$, $b^1\Sigma_0^+$ states are different from experimental values by 0.01 Å. The spectroscopic constants of the $A'\,^3\Delta_i$ and $A^3\Pi_i$ states, which have not yet been observed in experiment, are computed and listed for further comparison with experimental results.

**Table 3.** Computed and experimental spectroscopic constants of SeO.

| State | $T_e$/$cm^{-1}$ | | $\omega_e$/$cm^{-1}$ | | $B_e$/$cm^{-1}$ | | $r_e$/Å | |
|---|---|---|---|---|---|---|---|---|
| | Cal. | Exp. | Cal. | Exp. | Cal. | Exp. | Cal. | Exp. |
| $X_1^3\Sigma_0^-$ | 0 | 0[a] | 900.09 | 914.69[a] | 0.4694 | 0.4655[a] | 1.642 | 1.648[a] |
| $X_2\ ^3\Sigma_1^-$ | 96.3 | 165.9[a] | 899.94 | 915.43[a] | 0.4694 | 0.4738[a] | 1.642 | 1.633[a] |
| a $^1\Delta_2$ | 5813.2 | 5300[a] | 857.81 | – | 0.4627 | 0.461[a] | 1.653 | 1.65[a] |
| b $^1\Sigma_0^+$ | 10273.8 | 9723.5[b] | 808.81 | 838.8[b] | 0.4538 | 0.4560[b] | 1.670 | 1.665[b] |
| $A_1'\,^3\Delta_3$ | 23149.1 | – | 587.56 | – | 0.3473 | – | 1.909 | – |
| $A_2'\,^3\Delta_2$ | 23976.1 | – | 588.45 | – | 0.3477 | – | 1.908 | – |
| $A_3'\,^3\Delta_1$ | 24599.9 | – | 586.27 | – | 0.3452 | – | 1.914 | – |
| $A_1''\,^3\Sigma_1^+$ | 24815.8 | – | 587.20 | – | 0.3472 | – | 1.909 | – |
| $A_2''\,^3\Sigma_0^+$ | 24901.0 | – | 588.60 | – | 0.3454 | – | 1.914 | – |
| $A_1^3\Pi_0$ | 31259.1 | – | 388.85 | – | 0.3423 | – | 1.921 | – |
| $A_2^3\Pi_1$ | 31667.1 | – | 362.56 | – | 0.3418 | – | 1.925 | – |
| $A_3^3\Pi_2$ | 32100.0 | – | 342.83 | – | 0.3409 | – | 1.933 | – |

[a]Experimental values in Ref. [18], [b]experimental values in Ref. [19].

### 3.3. Electronic dipole transition moments and radiative lifetimes

The electronic dipole transition moments (TMs) of low-lying excited states are computed at SOC level. The transition moments for all states are fitted to a quartic polynomial function at an internuclear distance ranging from 1.29 Å to 3.6 Å. The average TMs in Franck–Condon region from the $X_2^3\Sigma_1^-$, $a^1\Delta_2$, $b^1\Sigma_0^+$, $A_1'^3\Delta_3$, $A_2'^3\Delta_2$, $A_3'^3\Delta_1$, $A_1^3\Pi_0$, $A_2^3\Pi_1$, $A_3^3\Pi_2$ states to the ground state $X_1^3\Sigma_0^-$ or $X_2^3\Sigma_1^-$ are shown in Table 4. For simplicity, we denote $X_1^3\Sigma_0^-$, $X_2^3\Sigma_1^-$ as $X_1$, $X_2$, respectively. The Franck–Condon factors for SeO from the $v'=0$ vibrational level of excited states to the $v''$ vibrational level of ground states ($X_1$ and $X_2$) are shown in Table 5. Since the FCFs from $v'=0$ to $v''=16$–21 are small, we neglect them in Table 5. In the a, b–X transitions, the FCF of $v'$–$v''$ ($v'=v''$) is the most intense. For the $a^1\Delta_2$ state, the maximum FCF is 0.97435 corresponding to 0–0 transition. The calculated 0–0 transition energy in a–$X_1$ transition is 5695.03 $cm^{-1}$, which is in agreement with early experimental value[4] within 495.03 $cm^{-1}$. For $b^1\Sigma_0^+$ state, the strongest transition to the ground state occurs at 0–0 with FCF being 0.8696. The computed 0–0 transition energy in $b^1\Sigma_0^+$–X is 10133.48 $cm^{-1}$, which is overestimated by 448 $cm^{-1}$ compared with early experimental result.[5] The radiative lifetimes of low-lying excited states are given in Table 6. Since the ground state X is split into two components ($X_1$ and $X_2$), we denote natural lifetimes for transitions from the $v'=0$ vibrational level of certain excited state to $X_1$ as $\tau_1$ and to $X_2$ as $\tau_2$, and the total natural lifetime of $v'=0$ as $\tau_{tot}$, and they are related to each other by

$$1/\tau_{tot} = 1/\tau_1 + 1/\tau_2. \quad (4)$$

The natural lifetime of $X_2$ derived from $X_2$–$X_1$ transition is $2.0\times10^6$ s. It is easily understood from this result that $X_2$ state is a stable state. The computed lifetime of $b^1\Sigma_0^+$ is 6.2 ms, which roughly accords in magnitude with the experimental value of 1.4 ms and other theoretical results of 4.7 ms[9] and 10.93 ms.[10] The calculated lifetime of $a^1\Delta_2$ is 0.14 s,

**Table 4.** Average transition dipole moments (in atomic units) in the Franck–Condon region.

| State | $X_2$ | $a^1\Delta_2$ | $b^1\Sigma_0^+$ | $c^1\Sigma_0^-$ | $A_2'^3\Delta_2$ | $A_1''^3\Sigma_1^+$ | $A_2''^3\Sigma_0^+$ |
|---|---|---|---|---|---|---|---|
| $X_1$ | $5.123\times10^{-4}$ | – | 0.0060 | – | – | 0.0084 | – |
| $X_2$ | – | 0.0045 | 0.0065 | 0.0120 | 0.0035 | 0.0353 | 0.0123 |

**Table 5.** Franck–Condon factors for transitions from the $v'=0$ vibrational energy levels of SeO excited electronic states to $v''=0$–15 and $v''=22$ vibrational energy levels of the ground states ($X_1$ and $X_2$).

| $v''$ | $a^1\Delta_2$–$X_2$ | $b^1\Sigma_0^+$–$X_1$ | $c^1\Sigma_0^-$–$X_2$ | $A_2'^3\Delta_2$–$X_2$ | $A_1''^3\Sigma_1^+$–$X_1$ | $A_2'^3\Sigma_0^+$–$X_2$ |
|---|---|---|---|---|---|---|
| 0 | $9.7435\times10^{-1}$ | $8.6960\times10^{-1}$ | $4.2210\times10^{-5}$ | $4.4051\times10^{-5}$ | $3.7272\times10^{-5}$ | $2.1338\times10^{-5}$ |
| 1 | $2.5328\times10^{-2}$ | $1.2190\times10^{-1}$ | $5.4617\times10^{-4}$ | $5.6517\times10^{-4}$ | $4.9227\times10^{-4}$ | $3.1568\times10^{-4}$ |
| 2 | $3.1784\times10^{-4}$ | $8.1647\times10^{-3}$ | $3.3620\times10^{-3}$ | $3.4492\times10^{-3}$ | $3.0928\times10^{-3}$ | $2.2197\times10^{-3}$ |
| 3 | $1.6198\times10^{-6}$ | $3.2549\times10^{-4}$ | $1.3141\times10^{-2}$ | $1.3360\times10^{-2}$ | $1.2314\times10^{-2}$ | $9.7970\times10^{-3}$ |
| 4 | $1.4704\times10^{-8}$ | $9.4409\times10^{-6}$ | $3.6500\times10^{-2}$ | $3.6819\times10^{-2}$ | $3.4781\times10^{-2}$ | $3.0133\times10^{-2}$ |
| 5 | $1.3053\times10^{-8}$ | $3.94612\times10^{-7}$ | $7.6260\times10^{-2}$ | $7.6517\times10^{-2}$ | $7.3773\times10^{-2}$ | $6.8031\times10^{-2}$ |
| 6 | $1.9806\times10^{-11}$ | $8.5302\times10^{-9}$ | $1.2438\times10^{-1}$ | $1.2449\times10^{-1}$ | $1.2194\times10^{-1}$ | $1.1699\times10^{-1}$ |
| 7 | – | $3.3768\times10^{-9}$ | $1.6271\times10^{-1}$ | $1.6277\times10^{-1}$ | $1.6135\times10^{-1}$ | $1.5825\times10^{-1}$ |
| 8 | – | $9.7013\times10^{-11}$ | $1.7412\times10^{-1}$ | $1.7419\times10^{-1}$ | $1.7436\times10^{-1}$ | $1.7339\times10^{-1}$ |
| 9 | – | $7.0961\times10^{-10}$ | $1.5459\times10^{-1}$ | $1.5456\times10^{-1}$ | $1.5615\times10^{-1}$ | $1.5781\times10^{-1}$ |
| 10 | – | $2.0962\times10^{-10}$ | $1.1511\times10^{-1}$ | $1.1493\times10^{-1}$ | $1.1729\times10^{-1}$ | $1.2165\times10^{-1}$ |
| 11 | – | $2.0329\times10^{-11}$ | $7.2467\times10^{-2}$ | $7.2211\times10^{-2}$ | $7.4532\times10^{-2}$ | $8.0266\times10^{-2}$ |
| 12 | – | $5.0466\times10^{-11}$ | $3.8798\times10^{-2}$ | $3.8560\times10^{-2}$ | $4.0322\times10^{-2}$ | $4.5463\times10^{-2}$ |
| 13 | – | – | $1.7752\times10^{-2}$ | $1.7561\times10^{-2}$ | $4.0322\times10^{-2}$ | $2.2064\times10^{-2}$ |
| 14 | – | – | $6.9715\times10^{-3}$ | $6.8385\times10^{-3}$ | $1.8649\times10^{-2}$ | $9.1205\times10^{-3}$ |
| 15 | – | – | $2.3578\times10^{-3}$ | $2.2854\times10^{-3}$ | $7.3965\times10^{-3}$ | $3.1924\times10^{-3}$ |
| ... | – | – | – | – | – | – |
| 22 | – | – | $1.5436\times10^{-8}$ | $8.3554\times10^{-9}$ | $2.361\times10^{-8}$ | $9.6762\times10^{-8}$ |

which is obviously less than other theoretical values 1.1 s[9] and 1.4 s.[10] This discrepancy results from the absence of magnetic transitions considered in this work. The radiative lifetimes (Table 6) for other low-lying states of the SeO molecule have not been obtained experimentally. However, the radiative lifetimes for these states of an isovalent TeO molecule have been computed in Ref. [20] with the LSC-SO-CI method. The computed lifetime for $c^1\Sigma_0^-$ state of the TeO molecule is 1.4 ms, whereas the calculated lifetime for $c^1\Sigma_0^-$ state of SeO is 0.9 ms, the lifetime for $c^1\Sigma_0^-$ state of SeO accords in magnitude with that of the TeO molecule. The computed lifetimes for $A_2'\,^3\Delta_2$, $A_1''\,^3\Sigma_1^+$, $A_2''\,^3\Sigma_0^+$ states of TeO are 1.9 ms, 8.1 μs, and 1.2 ms, respectively. Similarly, the calculated lifetimes for those states of SeO are 8 ms, 66 μs, and 0.58 ms, respectively. The lifetimes for $A_2'\,^3\Delta_2$ in SeO and in TeO molecules are both on the order of $10^{-3}$ s.

**Table 6.** Radiative lifetimes for transitions from the $v' = 0$ vibrational energy levels of SeO excited electronic states to the $X_1$ and $X_2$ states.

| State | $\tau_1$(s)–$X_1$ | $\tau_2$(s)–$X_2$ | $\tau_{\rm tot}$/s |
|---|---|---|---|
| $X_2{}^3\Sigma_1^-$ | $2.0\times10^6$ | – | $2.0\times10^6$ |
| $a^1\Delta_2$ | – | 0.14 | 0.14 |
| $b^1\Sigma_0^+$ | 0.013 | 0.011 | $6.2\times10^{-3}$ |
| $c^1\Sigma_0^-$ | – | $9\times10^{-4}$ | $9\times10^{-4}$ |
| $A_2'\,^3\Delta_2$ | – | $8\times10^{-3}$ | $8\times10^{-3}$ |
| $A_1''\,^3\Sigma_1^+$ | $1.2\times10^{-3}$ | $7.0\times10^{-5}$ | $6.6\times10^{-5}$ |
| $A_2''\,^3\Sigma_0^+$ | – | $5.8\times10^{-4}$ | $5.8\times10^{-4}$ |

# 4. Summary

The potential energy curves of SeO are computed with the MRCI+Q method. For better accuracy, the Ω-state potential energy curves of SeO with the inclusion of the spin–orbit coupling effects are also obtained by diagonalizing the Hamiltonian containing the spin–orbit pseudopotential operator in the basis of the Λ–S MRCI wavefunction. The electronic dipole transition moments from the low-lying excited states to the ground state are theoretically obtained. Subsequently, the radiative lifetimes for the $v' = 0$ vibrational level of low-lying states are calculated based on the fitted Ω-state potential energy curves and calculated electronic-dipole moments. The computed results in this paper are consistent with available experimental and other theoretical results. In addition, the spectroscopic data and transition properties which are absent in experiments are provided for further comparison.

# References


[1] Burling F T and Goldstein B M 1992 *J. Am. Chem. Soc.* **114** 2313

[2] Yan B, Pan S and Guo Q Q 2008 *Chin. Phys.* B **17** 3318

[3] Lee E P F, Mok D K W, Chau F and Dyke J M 2004 *J. Chem. Phys.* **121** 2962

[4] Fink E, Setzer K, Ramsay D and Vervloet M 1987 *J. Mol. Spectrosc.* **125** 66

[5] Winter R, Barnes I, Fink E H , Wildt J and Zabel F 1980 *Chem. Phys. Lett.* **73** 297

[6] Fan Q C, Sun W G, Li H D and Feng H 2012 *Chin. Phys.* B **21** 023301

[7] Zheng T, Qin J M, Jiang D Y, Lü J W and Xiao S C 2012 *Chin. Phys.* B **21** 043302

[8] Reddy S and Verma K 1980 *J. Mol. Spectrosc.* **84** 89

[9] Matsushita T, Klotz R, Marian C M and Peyerimhoff S D 1987 *Mol. Phys.* **62** 1385

[10] Chattopadhyaya S, Nath A and Das K K 2012 *Spectrochim. Acta* Part A **89** 160

[11] Werner H J, Knowles P J, Lindh R, Manby F R, SchÄutz M and others *MOLPRO–A Package of Ab Initio Programs* (version 2010.1) http://www.molpro.net

[12] Stoll H, Metz B and Dolg M 2002 *J. Comput. Chem.* **23** 767

[13] Bergner A, Dolg M, Küchle W, Stoll H and Preuß H 1993 *Mol. Phys.* **80** 1431

[14] Werner H J and Knowles P J 1988 *J. Chem. Phys.* **89** 5803

[15] Knowles P J and Werner H J 1988 *Chem. Phys. Lett.* **145** 514

[16] Langhoff S R and Davidson E R 1974 *Int. J. Quantum Chem.* **8** 61

[17] Le Roy R J 2002 *LEVEL* 7.5—*A Computer Program for Solving the Radial Schröinger Equation for Bound and Quasibound Levels* University of Waterloo, Chemical Physics Research Report CP-655

[18] Carrington A, Currie G N, Levy D H and Miller T A 1969 *Mol. Phys.* **17** 535

[19] Barrow R F and Lemanczyk R Z 1975 *Can. J. Phys.* **53** 553

[20] Rai-Constapel V, Liebermann H P, Buenker R J and Rai S N 2006 *J. Phys. Chem.* A **110** 404